Nonionic surfactant blends to control the size of microgels and their catalytic performance during glycoside hydrolyses

Babloo Sharma and Susanne Striegler*

Department of Chemistry and Biochemistry, 345 North Campus Drive, University of Arkansas, Fayetteville, Arkansas 72701, United States.

ABSTRACT: In a proof of concept study, a series of nonionic surfactant blends derived from Tween 80 and Span 80 was used to prepare catalytic microgels from stabilized droplets in miniemulsions. The goal of this study is to optimize the catalytic efficiency of the microgels by decreasing their particle size with surfactants that are custom-made for the respective pre-polymerization mixture. The effectiveness of the approach is examined by evaluating the catalytic efficiency of the resulting microgels in comparison to their counterparts made in presence of ionic SDS solution. Spherical particles with HLB value-dependent mean hydrodynamic diameters between 99 and 200 nm are obtained. Addition of Cu(II) ions and selected other transition metal ions activated the dormant catalysts for cleavage of glycosidic bonds in HEPES buffer at pH 7.00 and 37 °C using a fluorescent model substrate. The highest proficiency for the catalytic hydrolysis was observed for Cu(II)-containing microgels ($k_{cat}/K_M \times k_{non} = 870,000$) with the lowest diameter indicating an almost two-fold better stabilization of the transition state compared to a microgel prepared in presence of ionic SDS solution. The study establishes a correlation of HLB value of the nonionic surfactant blend used during material synthesis to the particle size and catalytic performance of the resulting microgels.

KEYWORDS: hydrophilic-lipophilic balance (HLB), nonionic surfactant, miniemulsion, macromolecular catalyst, hydrolysis, glycosides

1. Introduction.

Tremendous efforts are currently set forth to understand the role of polymer structures in catalysis by transition metal and metal oxide nanoparticle composites. ¹⁻³ The structures of polymers in these hybrid materials contribute in molecular recognition events, ⁴ drug delivery, ⁵ provide control of the stability of oil in water-emulsions, ⁶ and are used as probes for optical sensing and imaging. ⁷⁻⁸ Among such polymer-metal hybrid structures, microgels with immobilized transition metal complexes are of particular interest due to their flexibility in design and variety in potential applications. ⁹ The performance of microgels as catalytic entities is largely controlled by their architecture, ^{1, 10} which includes particle size, shape, matrix composition, ¹¹⁻¹³ nature of immobilized metal complex, ¹⁴ and the number of reaction sites. A method to precisely control the size of microgels prepared from miniemulsions is thus one of the most critical aspects for the rational design of particles with high catalytic efficiency.

In the miniemulsion polymerization methodology, the particle size is linearly dependent on the amount and nature of surfactants used during microgel synthesis. ¹⁵ In short, while the droplet size adjusts rapidly during ultra-sheering to approach a pseudo-steady state, it does not change during subsequent polymerization because of constant fusion and fission processes in hydrophobe-stabilized droplets. ¹⁵ The droplet surfaces are typically incompletely covered with surfactant molecules, and micelle formation does not occur in the continuous phase of miniemulsions. ¹⁵ Thus, for a given monomer mixture in a constant amount of aqueous layer, the size of the later microgel particle is directly dependent on the quality of the prepared miniemulsions and precisely controlled by the nature and amount of surfactant. ¹⁶⁻¹⁷ Therefore, the size of the microgels

is not influenced by the progress of the polymerization itself. Instead, the employed hydrophobic agent prevents or slows down premature Ostwald ripening of generated droplets in the miniemulsion after ultrasonication and allows polymerization as is.¹⁸ The equality of droplet pressure makes such systems insensitive to net mass exchange by diffusion processes when a minimum molar ratio of hydrophobe to monomer of approximately 1 to 250 is maintained.¹⁹ Droplet growth of such stabilized miniemulsions occurs on the timescale of hundreds of hours.¹⁹

Along these lines, our initial attempts to decrease the particle size of previously prepared catalytic microgels focused on increasing the amount of ionic sodium dodecyl sulfate surfactant in pre-polymerization mixtures. However, the mean hydrodynamic diameters (Dh) of the resulting microgels decreased only slightly from 293 nm at 17 mM to 241 nm in 120 mM SDS solution (see Supporting Information). Thus, changing the nature of the surfactant by using nonionic instead of ionic surfactants appears as a promising strategy to overcome the encountered pitfall. Nonionic surfactants show several intrinsic advantages over their ionic counterparts. Based on a given surfactant blend with defined hydrophilic-lipophilic balance (HLB), 20 a large range of droplet properties can be designed, such as size, transparency, homogeneity, and the overall stability of a miniemulsion. We describe below custom-made blends of nonionic surfactants that are optimized for the composition of pre-polymerization mixtures in selected miniemulsions. The effectiveness of the approach was examined by evaluating the catalytic efficiency of the resulting microgels in comparison to their counterparts made in presence of ionic SDS solution.

2. Results and Discussion

2.1 Synthesis of microgels in presence of nonionic surfactant blends

To identify a suitable surfactant blend for the envisaged microgel synthesis, blends of hydrophilic Tween 80 and hydrophobic Span 80 (Chart 1) are prepared between HLB 4.3 (100% Span 80) and 15.0 (100% TWEEN 80) by mixing corresponding amounts of the separate surfactants. The HLB values of the resulting blends are calculated from the wt % of the used surfactants and their respective HLB values (eq. 1).²¹

$$HLB_{blend} = wt\%_{Tween 80} \times 15.0 + wt\%_{Span 80} \times 4.3$$
 (eq.1)

To prepare the microgels, a mixture of the crosslinker ethyleneglycol dimethacrylate (EGDMA (1), 60 mol%), the monomer butyl acrylate (BA (2), 40 mol%) and a pentadentate ligand (VBbsdpo, (3), 0.5 mol%) in aqueous CAPS buffer is added to the selected surfactant blend (Chart 2, Scheme 1). Subsequently, hexadecane is added to the reaction mixture as a stabilizing hydrophobe to prevent Ostwald-ripening of the formed droplets; aliquots of aqueous Cu(II) acetate solutions are then added to prepare the Cu₂VBbsdpo catalyst (Cu₂L; L = VBbsdpo, (3)) *in-situ*; and, finally, mannose (4) is added as a coordinating counter anion after deprotonation to prevent premature leaking of Cu(II) ions from the complex during material synthesis. 12

Miniemulsions of the pre-polymerization mixtures are obtained by ultra-sheering with a sonication horn. The generated droplets are captured as microgels by free-radical polymerization over 60 min in the cold. The reaction is initiated by 2,2'-dimethoxy-2-phenylacetophenone (5) under UV light. For subsequent analyses of particle sizes, the excess of nonionic surfactant is removed by extracting the aqueous dispersions with dichloromethane.

2.2 Determination of the particle size by dynamic light scattering

The mean hydrodynamic diameter (D_h) of the synthesized particles is determined by dynamic light scattering of 1250-fold diluted dispersions of the extracted gels in nanopure water. A correlation between particle size and polarity of the surfactant blend is obtained that is linked to the HLB value of the nonionic surfactant blend used during material synthesis (**Fig. 1**). The analysis reveals HLB value-dependent sizes of the microgels between 99 and 200 nm. Surfactant blends with a HLB of 10.9 stabilize the miniemulsions best and yield microgels of the smallest size and a mean hydrodynamic diameter (D_h) of 99 nm. For comparison, microgels with similar composition prepared in presence of ionic SDS show a

Chart 1. Structures of Tween 80 and Span 80

Chart 2. Structures of key compounds in the prepolymerization mixture

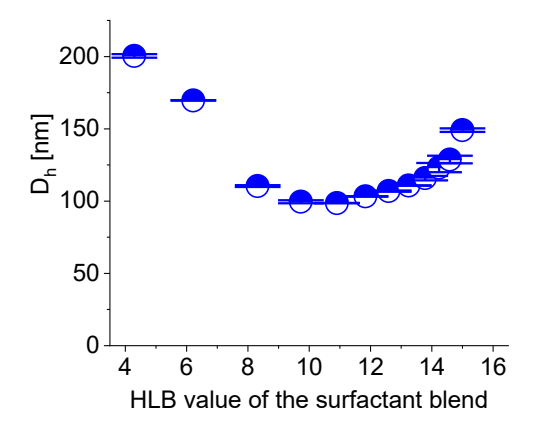


Fig. 1. Hydrodynamic diameter of microgels prepared in the presence nonionic surfactant blends

Scheme 1. Protocol for microgel synthesis and evaluation in presence of nonionic surfactant blends.



hydrodynamic diameter of 252 nm (see Supporting Information). While HLB values between 4 and 6 are best suited for miniemulsions of water in oil (W/O), they provide poor particle dispersions in water as apparent by the large resulting diameter of the corresponding microgels prepared under these conditions (110-200 nm, **Fig. 1**). By contrast, miniemulsions of oil in water are generally stable for HLB values above 7,²²⁻²³ and result in overall smaller particles for the microgels under investigation here (99-149 nm, **Fig. 1**).

2.3 Particle morphology imaged by transmission electron microscopy

A few drops of the extracted microgel dispersions at HLB 10.9 were placed on Cu grids after dilution with nanopure water and allowed to dry at ambient temperature. Transmission electron microscopy shows the gels as spherical particles (**Fig. 2**). The analysis of an image with 564 particles (see Supporting Information) reveals the mean diameter of microgels prepared at HLB 10.9 as 95.3 \pm 0.8 nm (**Fig. 3**). Agglomerated particles caused by the removal of surfactant are excluded in the analysis. Thus, the particles in the dry state are only slightly smaller than in solution (D_h = 99 nm, see above). Consequently, the crosslinked microgels do not swell to a significant extent in water and are not popcorn-like as observed previously. $^{11,\,24}$

2.4 Amount of immobilized metal complex determined by gravimetric analysis

Prior to an analysis of the performance of the synthesized microgels during the hydrolysis of glycosidic bonds, the concentration of immobilized catalyst has to be known. This task has been previously achieved reliably and reproducably for microgels prepared in presence of ionic SDS by determining the nitrogen content of the microgel using elemental analysis. ¹¹⁻¹³,

²⁵ The nitrogen content is directly related to the amount of the immobilized pentadentate ligand amount. However, the nitrogen content of the microgels prepared here is twice as low due to a change of the immobilized ligand and close to the detection limit of the methodology. Additionally, a blend of Tween 80 and Span 80 cannot be removed from the microgels via dialysis due to the intrinsic features of the selected surfactants. Therefore, we followed the microgel formation by gravimetric analysis and determined the ligand concentration in the obtained microgels from the polymerization proceedings at 60 min assuming equal polymerization of all functional monomers. Along these lines, microgels prepared at HLB values 10.9, 13.8 and 15 were chosen as representative examples. Typically, 100 µL aliquots of the reaction mixtures are taken in regular time intervals, treated with pyrocatechol to stop the radical polymerization, and then heated to remove all volatile components. The remaining weight of the samples is corrected for contributions from surfactants and non-removable solids prior to analysis (Fig. 4). After 60 min, the proceedings of the polymerizations are highest at HLB 10.9 (69%), and somewhat lower at HLB 13.8 (60 %) and 15 (53 %). The ligand concentration is 0.56 mM in microgels prepared at HLB 10.9; 0.49 mM at HLB 13.8; and 0.43 mM at HLB 15. Interestingly, the hydrodynamic diameters of the particles in the respective dispersions increase in reversed order, i.e. 99 nm (HLB 10.9) < 116 nm (HLB 13.8) < 149 nm (HLB 15) (Fig. 1). Thus, the yield and the size of the particles in the resulting microgel dispersions are both dependent on the HLB value of the surfactant blends used for material synthesis.

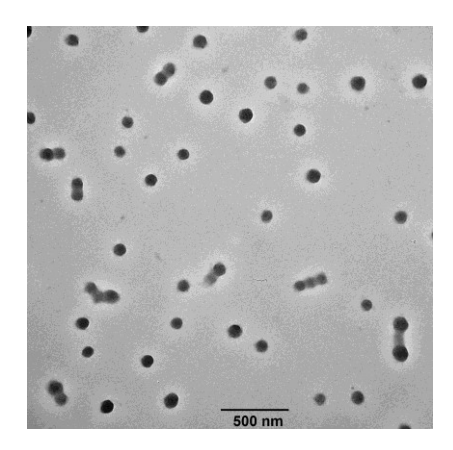


Fig. 2. TEM image of microgel particles prepared at HLB 10.9

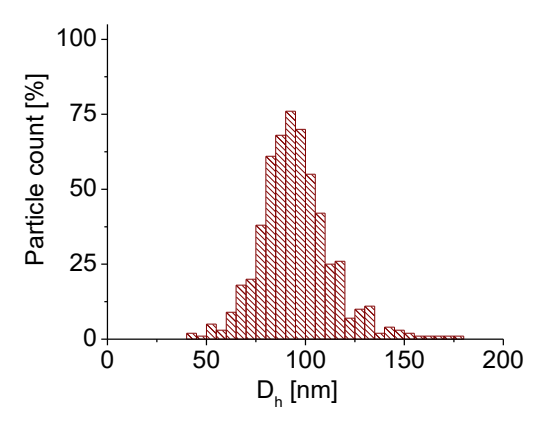


Fig. 3. Distribution of microgel diameters at HLB 10.9

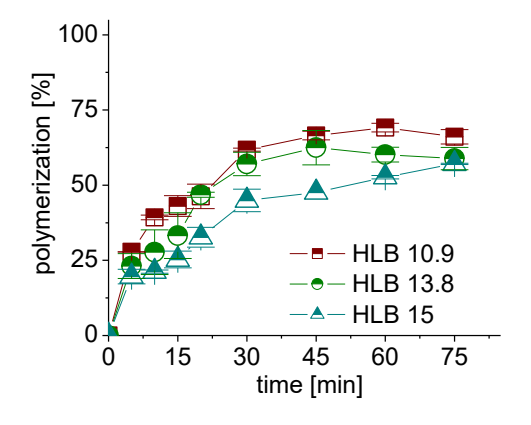


Fig. 4, Gravimetric analysis of microgel formation in presence of non-ionic surfactant blends.

In control experiments, the nonionic surfactant blend is replaced by SDS solution in otherwise identical prepolymerization mixtures yielding 66% transformation of polymerizable monomers after 60 min (data not shown). The ligand concentration of these polymers is 0.58 mM and determined as described above. The yields of the microgels synthesized in presence of the nonionic surfactant blend at HLB 10.9 and of ionic SDS are hence comparable, while their diameters are different, i.e. 99 nm in the Tween 80-Span 80 surfactant blend and 252 nm in the aqueous SDS solution.

2.5 Catalytic performance of microgels prepared in presence of nonionic surfactant blends

With an experimentally determined concentration of the immobilized VBbsdpo ligand on hand, 1 mL aliquots of the synthesized microgel dispersions are dialyzed against nanopure water to remove low molecular weight compounds and nonpolymerized monomers. The purified polymer dispersions with the dormant catalyst are then diluted into 10 mL with aqueous 50 mM CAPS buffer, activated by addition of appropriate amounts of metal ions and used in 20 μ L aliquots as elaborated previously. ^{12, 25} All kinetic assays are performed in 96-well plates in aqueous 50 mM HEPES buffer solution at pH 7 and at 37°C using 4-methylumbelliferyl N-acetyl-β-Dglucosaminide (6) as a model substrate (Scheme 2). The hydrolytic cleavage of 6 leads to formation of 4methylumbelliferone (7) that can be quantified by fluorescence spectroscopy after excitation at 360 nm and recorded emission at 465 nm. The analysis of the time-dependent emission recordings for the catalyzed hydrolyses of 6 under steadystate conditions allows deducing of kinetic parameter after application of the Michaelis-Menten model.

All microgels activated with Cu(II) ions catalyze the substrate hydrolysis with comparable rate constants ($k_{\rm cat}$) (**Table 1**). By contrast, the affinity ($K_{\rm M}$) for catalytic sites in those gels rises with increasing polarity of the surfactant blend employed during material synthesis, i.e from HLB 10.9, 13.8, and 15 to ionic SDS solution. Consequently, the efficiency ($k_{\rm cat}/K_{\rm M}$) of the resulting catalysts decreases in the same order. Correlating the hydrodynamic diameter ($D_{\rm h}$) of the microgels (**Fig. 5**) to kinetic data suggests the highest catalytic proficiency for the microgel with the smallest particle size (HLB 10.9).

Scheme 2. Catalytic hydrolysis of substrate 6

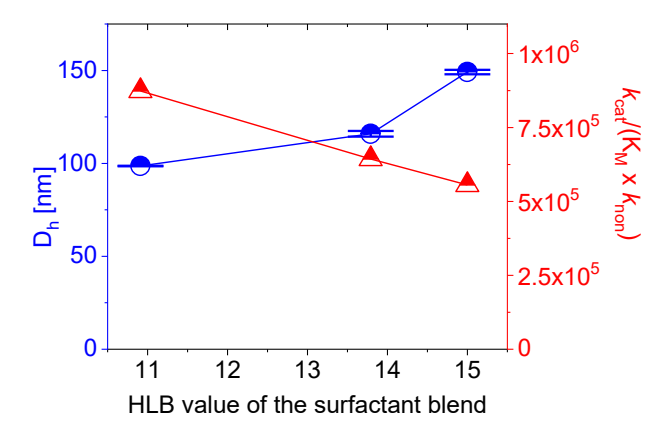


Fig. 5. Catalytic proficiency and particle size as a function of the HLB value used during microgel synthesis

Table 1. Kinetic parameter and catalytic proficiency for the catalytic hydrolysis of 6 in 50 mM HEPES buffer at pH 7.0 and $37~^{\circ}\text{C}$ by Cu₂VBbsdpo-containing microgels relative to their size and the HLB value of the surfactant blend used during synthesis

Entry	HLB	$D_h \pm \Delta D_h [nm]$	$k_{\rm cat} \pm \Delta k_{\rm cat} \times 10^{-4} [\rm min^{-1}]$	$K_{\rm M} \pm \Delta K_{\rm M} [{\rm mM}]$	$k_{\rm cat}/[{ m K_M} \times k_{ m non}]$
1	10.9	99 ± 1	6.0 ± 0.4	2.6 ± 0.8	870,000
2	13.8	116 ± 2	5.9 ±0.3	3.5 ± 0.6	640,000
3	15	149 ± 1	6.3 ± 0.4	4.3 ± 0.2	560,000
4	SDS	252 ± 4	6.1 ± 0.1	4.5 ± 0.5	520.000

 $^{^{}a}k_{\text{non}} = 2.6 \times 10^{-7} \text{ min}^{-1} \text{ M}^{-1}$

Table 2. Kinetic parameter and catalytic proficiency for the catalytic hydrolysis of 6 in 50 mM HEPES buffer at pH 7.0 and 37 °C by VBbsdpo-containing microgels prepared at HLB 10.9 and activated with different metal ion acetates

Entry	M^{z^+}	$k_{\rm cat} \pm \Delta k_{\rm cat} \times 10^{-4} [\rm min^{-1}]$	$K_{\rm M} \pm \Delta K_{\rm M} [mM]$	$k_{\rm cat}/{\rm K_M[min^{-1}M^{-1}]}$	$k_{\rm cat}/{\rm K_M} \times k_{\rm non}$
1	Cu(II)	6.0 ± 0.4	2.6 ± 0.8	0.230	870,000
2	Ni(II)	4.7 ± 0.6	3.1 ± 0.8	0.150	590,000
3	Zn(II)	6.4 ± 0.6	4.2 ± 0.7	0.150	580,000

 $^{^{}a}k_{non} = 2.6 \times 10^{-7} \text{ min}^{-1} \text{ M}^{-1}$

Encouraged by the results, a microgel prepared at HLB 10.9 was activated in-situ with Zn(II) and Ni(II) ions to determine the performance of the resulting catalysts toward the model reaction. The bsdpo ligand motif is known to bind various Lewis-acidic metal ions, e.g. Cu(II), Zn(II), Ni(II), Mn(III) and Fe(III). 26-37 Therefore, the complex formation in the waterdispersed microgel is quantified by isothermal titration calorimetry (ITC) using the gravimetrically determined concentration of the ligand (0.11 mM) upon titration with aqueous 20 mM metal ion acetate solutions. Interestingly, the titration shows an exothermic formation of Cu(II) species, while the activation of the dormant catalysts with Ni(II) and Zn(II) ions is endothermic (Figures S4-S6). In more details, the titration of the dialyzed metal-free microgel with aqueous Cu(II) acetate solution confirmed the formation of a binuclear Cu(II) complex within the microgel upon addition of two mol equivalents of Cu(II) ions per mol of immobilized ligand (Figure S4). The binuclear M_2L motif $(L = bsdpo)^{31}$ of the Cu(II) complex is typically preserved in aqueous solution. 26-27 Thus, the titrated Cu(II) ions are likely to occupy a square planar geometry upon coordination to the immobilized pentadentate ligand. 26-27 At pH 10.5, a hydroxyl ion is shown to coordinate as a terminal ligand to one of the two Cu(II) centers in the low molecular weight complex, while the other free coordination site is occupied by water accounting for two different binding sites. 31, 38

Upon titration of the metal ion-free microgel with Ni(II) ions, the formation of a similar binuclear species is apparent (**Figure S5**). Binuclear low molecular weight complexes derived from the bsdpo ligand and Ni(II) ions are described for the solid state. In contrast to the terminal hydroxyl group observed in the bsdpo-Cu(II) complex, the hydroxyl ion in the bsdpo-Ni(II) complex bridges the metal core and thus has a lower nucleophilicity. Therefore, the microgel activated with Cu(II) ions is more efficient in hydrolyzing the glycosidic bond of the model substrate **6** than a microgel catalyst derived from Ni(II) ions (**Table 2**, Entries 1 and 2). The combined observations imply that the described structural features of the Cu(II) and Ni(II) species are preserved in the *in-situ* generated complexes in the microgel catalysts.

When activating the dormant catalyst with Zn(II) ions, incomplete saturation of the metal binding sites in the immobilized VBbsdpo ligand is evident (Figure S6). The titration data imply the formation of a mono- instead of a binuclear Zn(II) species in the microgel. The obtained ITC data are in line with the noted preference of the pentadentate bsdpo ligand to form mono- instead of binuclear Zn(II) species in solution that utilize a N₂O₂ instead of a N₂O₃ set of donor atoms.²⁹ The nucleophilic hydroxyl ion is suggested to bind as terminal ligand in the apical position of a tetrapyramidal geometry around the Zn(II) ion.²⁹ However, a higher catalytic activity of bi- over mononuclear catalysts is observed by us and others on different occasion previously. ³⁰⁻³² Thus, a lower catalytic activity of microgels activated with Zn(II) ions in comparison to those activated with Cu(II) ions results (Table 2, Entries 1 and 3). Consequently, the efficiency of the dormant microgel catalysts is overall highest when activated with Cu(II) ions, and lower when activated with Ni(II) and Zn(II) ions despite their notable Lewis-acidity.

Conclusions

The use of non-ionic surfactant blends during the synthesis of catalytic microgels from hydrophobe-stabilized miniemulsions allows a rational design of the particle size by selection of the hydrophilic-lipophilic balance of the applied surfactant blend. As a result, the particle size of microgels derived from miniemulsions of EGDMA, BA and pentadentate ligand VBbsdpo is reduced by 2.5-fold. The mean hydrodynamic diameter for microgels prepared in ionic SDS solution is 252 nm, and 99 nm for their counterparts prepared at HLB 10.9 in Tween 80-Span 80 solutions. The latter microgel dispersions contain spherical instead of popcorn-like particles that only slightly swell in aqueous solution.

When activating the dormant catalysts with Cu(II) ions, a catalytic proficiency of 870,000 results for microgels with the smallest particle size. Larger particles are less efficient at comparable rate constants due to increased substrate affinity. The stabilization of the transition state (K_{TS}), which is reciprocal to the catalytic proficiency, calculates as 1.15×10^{-6} , which is almost twice as good as that observed for microgels prepared in ionic SDS solution. Activation of the dormant microgels with Ni(II) and Zn(II) ions yields less proficient catalysts. Overall, our approach explores a new promising direction for biomimetic catalysis by optimizing the surfactant applied during formulation of droplets and miniemulsions to the composition and envisaged properties of the resulting material.

ASSOCIATED CONTENT

AUTHOR INFORMATION

Corresponding Author

*Email: <u>Susanne.Striegler@uark.edu</u>; phone: +1-479-575-5079; fax: +1-479-575-4049.

ORCID

Babloo Sharma: 0000-0002-0265-322X Susanne Striegler: 0000-0002-2233-3784

Author Contributions

The manuscript was written through contributions of all authors. All authors have given approval to the final version of the manuscript

ABBREVIATIONS

CAPS, N-cyclohexyl-3-aminopropanesulfonic acid; HEPES, 2-[4-(2-hydroxyethyl)piperazin-1-yl]ethanesulfonic acid; D_h , mean hydrodynamic diameter; DLS, dynamic light scattering; ITC, isothermal titration calorimetry; TEM, transmission electron microscopy.

Supporting Information. Experimental details of the microgel synthesis in presence of nonionic surfactant blends, DLS and TEM analysis, kinetic assays, and isothermal titrations. This material is available free of charge via the Internet at http://pubs.acs.org.

ACKNOWLEDGMENT

Support of this research to S. S. by the National Science Foundation (CHE-1854304), and the Arkansas Biosciences Institute are gratefully acknowledged.

REFERENCES

- 1. Shifrina, Z. B.; Matveeva, V. G.; Bronstein, L. M. Role of Polymer Structures in Catalysis by Transition Metal and Metal Oxide Nanoparticle Composites. Chem. Rev. 2020, 120, 1350-1396.
- 2. Plamper, F. A.; Richtering, W. Functional Microgels and Microgel Systems. Acc. Chem. Res. 2017, 50, 131-140.
- 3. Wiese, S.; Spiess, A. C.; Richtering, W. Microgel-Stabilized Smart Emulsions for Biocatalysis. Angew. Chem., Int. Ed. 2013, 52, 576-579.
- 4. Li, F.; Lyu, D.; Liu, S.; Guo, W. DNA Hydrogels and Microgels for Biosensing and Biomedical Applications. Adv. Mater. 2020, 32, 1806538.
- 5. Smeets, N. M. B.; Hoare, T. Designing responsive microgels for drug delivery applications. J. Polym. Sci. Pol. Chem. 2013, 51, 3027-3043.
- 6. Brugger, B.; Richtering, W. Magnetic, Thermosensitive Microgels as Stimuli-Responsive Emulsifiers Allowing for Remote Control of Separability and Stability of Oil in Water-Emulsions. Adv. Mater. 2007, 19, 2973-2978.
- 7. Sierra-Martin, B.; Fernandez-Barbero, A. Inorganic/polymer hybrid nanoparticles for sensing applications. Adv. Colloid Interface Sci. 2016, 233, 25-37.
- 8. Battista, E.; Causa, F.; Netti, A. P. Bioengineering Microgels and Hydrogel Microparticles for Sensing Biomolecular Targets. Gels 2017, 3, 20.
- 9. Landfester, K. Miniemulsion Polymerization and the Structure of Polymer and Hybrid Nanoparticles. Angew. Chem., Int. Ed. 2009, 48, 4488-4507.
- 10. Antonietti, M.; Landfester, K. Polyreactions in miniemulsions. Prog. Polym. Sci. 2002, 27, 689-757.
- 11. Sharma, B.; Striegler, S. Crosslinked Microgels as Platform for Hydrolytic Catalysts. Biomacromolecules 2018, 19, 1164–1174.
- 12. Sharma, B.; Striegler, S.; Whaley, M. Modulating The Catalytic Performance Of An Immobilized Catalyst With Matrix Effects A Critical Evaluation. ACS Catal. 2018, 8, 7710-7718.
- 13. Sharma, B.; Striegler, S. Tailored Interactions of the Secondary Coordination Sphere Enhance the Hydrolytic Activity of Cross-Linked Microgels. ACS Catal. 2019, 9, 1686-1691.
- 14. Striegler, S.; Dittel, M.; Kanso, R.; Alonso, N. A.; Duin, E. C. Hydrolysis of Glycosides with Microgel Catalysts. Inorg. Chem. 2011, 50, 8869-8878.
- 15. Landfester, K.; Bechthold, N.; Tiarks, F.; Antonietti, M. Formulation and Stability Mechanisms of Polymerizable Miniemulsions. Macromolecules 1999, 32, 5222-5228.
- 16. Antonietti, M.; Landfester, K. Polyreactions in miniemulsions. Progr. Polym Sci. 2002, 27, 689-757.
- 17. Bechthold, N.; Tiarks, F.; Willert, M.; Landfester, K.; Antonietti, M. Miniemulsion polymerization: applications and new materials. Macromolecular Symposia 2000, 151, 549-555.
- 18. Landfester, K. Synthesis of colloidal particles in miniemulsions. Ann. Rev. Mat. Res. 2006, 36, 231-279.
- 19. Kabalnov, A. S.; Pertzov, A. V.; Shchukin, E. D. Ostwald ripening in emulsions: I. Direct observations of Ostwald ripening in emulsions. J. Coll. Interf. Sci. 1987, 118, 590-597.
- 20. Griffin, W. C. Classification of Surface-Active Agents by "HLB". J. Cosmet. Sci. 1949, 1, 311-326.
- 21. Griffin, W. C. Calculation of HLB values of non-ionic surfactants. J. Soc. Cosmet. Chem. 1954, 5, 249-256.
- 22. Pichot, R.; Spyropoulos, F.; Norton, I. T. O/W emulsions stabilised by both low molecular weight surfactants and colloidal particles: The effect of surfactant type and concentration. J. Colloid Interf. Sci. 2010, 352, 128-135.
- 23. A. Bos, M.; van Vliet, T. Interfacial rheological properties of adsorbed protein layers and surfactants: a review. Adv. Colloid Interface Sci. 2001, 91, 437-471.
- 24. Ocepek, M.; Soucek Mark, D.; Berce, P.; Meng, L. Comparison of Particle Size Techniques to Investigate Secondary Nuclea-

- tion in HEMA-Rich Latexes. Macromol. Chem. Phys. 2015, 216, 400-416.
- 25. Sharma, B.; Pickens, J. B.; Striegler, S.; Barnett, J. D. Biomimetic Glycoside Hydrolysis by a Microgel Templated with a Competitive Glycosidase Inhibitor. ACS Catal. 2018, 8, 8788–8795.
- 26. Mazurek, W.; Bond, A. M.; Murray, K. S.; O'Connor, M. J.; Wedd, A. G. Preparation and spectral, magnetic, and electrochemical characterization of a flexible phenoxo-bridged binuclear copper(II) complex. Inorg. Chem. 1985, 24, 2484-90.
- 27. Mazurek, W.; Berry, K. J.; Murray, K. S.; O'Connor, M. J.; Snow, M. R.; Wedd, A. G. Magnetic interactions in metal complexes of pentadentate binucleating ligands. 1. Synthesis and properties of binuclear copper(II) compounds containing single-atom-bridging ligands. Crystal and molecular structure of a binuclear .mu.-hydroxobridged copper(II) complex of 1,5-bis[1-(pyridin-2-yl)ethylideneamino]pentan-3-ol. Inorg. Chem. 1982, 21, 3071-3080.
- 28. Mazurek, W.; Bond, A. M.; O'Connor, M. J.; Wedd, A. G. Comparison of the electrochemical reduction of pentadentate binucleated nickel(II) and copper(II) compounds in dimethylformamide. Inorg. Chem. 1986, 25, 906-915.
- 29. Pal, C. K.; Mahato, S.; Joshi, M.; Paul, S.; Roy Choudhury, A.; Biswas, B. Transesterification activity by a zinc(II)-Schiff base complex with theoretical interpretation. Inorg. Chim. Acta 2020, 506, 119541.
- 30. Striegler, S.; Dittel, M. A Sugar's Choice: Coordination to a Mononuclear or a Dinuclear Copper(II) Complex? Inorg. Chem. 2005, 44, 2728-2733.
- 31. Striegler, S.; Dunaway, N. A.; Gichinga, M. G.; Barnett, J. D.; Nelson, A.-G. D. Evaluating Binuclear Copper(II) Complexes for Glycoside Hydrolysis. Inorg. Chem. 2010, 49, 2639-2648.
- 32. Vichard, C.; Kaden, T. A. Phosphate and phosphonate ester hydrolysis promoted by dinuclear metal complexes. Inorg. Chim. Acta 2002, 337, 173-180.
- 33. Bonadies, J. A.; Kirk, M. L.; Lah, M. S.; Kessissoglou, D. P.; Hatfield, W. E.; Pecoraro, V. L. Structurally diverse manganese(III) Schiff base complexes: chains, dimers, and cages. Inorg. Chem. 1989, 28, 2037-2044.
- 34. Bonadies, J. A.; Maroney, M. J.; Pecoraro, V. L. Structurally diverse manganese(III) Schiff base complexes: solution speciation via paramagnetic proton NMR spectroscopy and electrochemistry. Inorg. Chem. 1989, 28, 2044-2051.
- 35. Bertoncello, K.; Fallon, G. D.; Murray, K. S.; Tiekink, E. R. T. Manganese(III) complexes of a binucleating Schiff-base ligand based on the 1,3-diaminopropan-2-ol backbone. Inorg. Chem. 1991, 30, 3562-3568.
- 36. Fallon, G. D.; Markiewicz, A.; Murray, K. S.; Quach, T. A doubly bridged binuclear iron(III) complex containing inequivalent metal environments. Synthesis, structure and magnetism. J. Chem. Soc., Chem. Commun. 1991, 198-200.
- 37. Biswas, B.; Mitra, M.; Adhikary, J.; Rama Krishna, G.; Bag, P. P.; Reddy, C. M.; Aliaga-Alcalde, N.; Chattopadhyay, T.; Das, D.; Ghosh, R. Synthesis, X-ray structural and magnetic characterizations, and epoxidation activity of a new bis(μ-acetato)(μ-alkoxo)dinuclear iron(III) complex. Polyhedr. 2013, 53, 264-268.
- 38. Striegler, S. Discrimination of epimeric disaccharides by templated polymers. Anal. Chim. Acta 2005, 539, 91-95.

Graphical abstract:

